Analytical Methods

ROYAL SOCIETY OF CHEMISTRY

PAPER

Cite this: *Anal. Methods*, 2023, **15**, 297

Study on direct identification of bacteria by laser-induced breakdown spectroscopy

Ziqi Mi,[ab] Shuqing Wang,[c] Xiaofei Ma,[d] Yan Zhang,[e] Jiahui Liang,[ab] Fei Chen,[ab] Lei Zhang,[*ab] Gang Wang,[d] Wanfei Zhang,[d] Zhenrong Liu,[d] Xuebin Luo,[d] Zefu Ye,[f] Zhujun Zhu,[f] Wangbao Yin*[ab] and Suotang Jia[ab]

Bacteria are everywhere in the natural environment. Although most of them are harmless, there are still some hazardous bacteria that will harm human health, so it is particularly important to identify bacteria quickly. Compared with traditional time-consuming and complicated identification methods, laser-induced breakdown spectroscopy (LIBS) is one of the potential technologies for rapid identification of bacteria. In this paper, six weakly active bacteria, including *Escherichia coli*, *Enterococcus faecalis*, *Bacillus megaterium*, *Bacillus thuringiensis*, *Pseudomonas aeruginosa* and *Bacillus subtilis*, are taken as analysis samples. The thawed bacteria are placed in deionized water, and then uniformly smeared on five kinds of substrates to verify the feasibility of using LIBS to identify these bacteria. Spectrum filtering, normalization and principal component analysis (PCA) are used to preprocess the spectra, and a multi-class identification method based on the one-against-all linear kernel function of support vector machine (SVM) is proposed to establish the prediction model. The identification performance is evaluated by using precision and recall. The experimental results show that high-purity graphite is the best substrate with the least interference to the LIBS spectrum of bacteria. The prediction precision of these six bacteria is 77.27%, 92.86%, 84.21%, 94.12%, 81.82% and 76.92%, respectively, recall is 85%, 100%, 94.12%, 80%, 81.82% and 75% respectively, and the identification rate is 84.17%. It can be seen that the direct identification of bacteria can be preliminarily realized by smearing bacteria on the graphite substrate and analyzing its LIBS spectra, which provides a feasible way for simple, rapid and on-site bacterial identification.

Received 8th November 2022
Accepted 8th December 2022

DOI: 10.1039/d2ay01840c

rsc.li/methods

1 Introduction

In recent years, for the sake of safety, bacteria and other microorganisms have received more and more attention. Although most bacteria are beneficial to humans and the environment, there are still a few harmful or even hazardous bacteria that can cause plant wilting or human food poisoning. Therefore, rapid identification of bacteria is very important for timely and effective decontamination. Traditional identification generally relies on morphological identification, which includes the culture method, staining method and simple biochemical tests, such as observation of colony appearance characteristics, Gram-staining, spore staining and the catalase method. These methods are simple and easy to use, but they are only applicable to cultured organisms *in vitro*, and the identification rate is poor. The methods of bacterial identification developed in recent years, such as polymerase chain reaction[1] and 16S rDNA,[2] can clarify the genetic relationship between bacteria quickly and accurately in essence, but they require a variety of reagents, expensive instruments, highly professional skills and time-consuming sample preparation, so they cannot be used for field analysis. At present, the rapid methods of bacterial identification include Raman spectroscopy[3–5] and hyperspectral spectroscopy,[6] but the former has high requirements for the culture conditions and preparation process of bacteria, while in the latter it is difficult to select a characteristic wavelength that varies with the kind of bacteria.

Laser-induced breakdown spectroscopy (LIBS) uses a high-energy pulsed laser to focus on the sample surface for ablation to generate plasmas. By analyzing the spectral information of plasma radiation, such as the wavelength and intensity, the sample can be identified and classified. LIBS is a qualitative and semi-quantitative rapid analysis technique[7] with simple operation, few sample preparation and almost no damage,[8,9] and has

[a]State Key Laboratory of Quantum Optics and Quantum Optics Devices, Institute of Laser Spectroscopy, Shanxi University, Taiyuan, China. E-mail: k1226@sxu.edu.cn; ywb65@sxu.edu.cn
[b]Collaborative Innovation Center of Extreme Optics, Shanxi University, Taiyuan, China
[c]SINOPEC Research Institute of Petroleum Processing Co., Ltd., Beijing, China
[d]Shanxi Xinhua Chemical Defense Equipment Research Institute Co., Ltd., Taiyuan, China
[e]School of Optoelectronic Engineering, Xi'an Technological University, Xian, China
[f]Shanxi Gemeng US-China Clean Energy R&D Center Co., Ltd., Taiyuan, China

potential to be used to identify bacteria. Baudelet *et al.* used femtosecond LIBS (femto-LIBS) to establish a microelement hyperspace based on the concentrations of Na, Mg, P, K and Ca. *Acinetobacter baylyi*, *Bacillus subtilis*, *Erwinia chrysanthemi*, *Escherichia coli* and *Shewanella oneidensis* were classified after lyophilizing treatment and it was found that the discrimination ability was enhanced with the increase of the dimension of hyperspace.[10] Baudelet *et al.* performed experiments with femtosecond laser and nanosecond laser, and found that femto-LIBS is more sensitive to molecular bonds and can measure the CN bond released by bacteria.[11] J. Rehse *et al.* studied the effect of nutrient media on LIBS identification, and found that the cell membrane integrity of *Pseudomonas aeruginosa* cultured on a MacConkey plate containing bile salts was disrupted, and the identification of specific bacteria was better than that on trypticase soy agar (TSA) and blood agar plate.[12] R. Gamble *et al.* tried to change the water sources for bacterial isolation and culture by using deionized water, tris(hydroxymethyl)aminomethane (TRIS) buffered water, phosphate buffered saline water and reverse osmosis water, and found that the first two were better.[13] Marcos-Martinez *et al.* directly extracted *Pseudomonas aeruginosa*, *Escherichia coli* and *Salmonella typhimurium* from the frozen culture and grew them on common Petri dishes, and then the identification certainty of LIBS was 95%.[14] Zhao *et al.* used principal component analysis (PCA) and genetic algorithm (GA) to select spectral features and compress data, and established artificial neural network (ANN) and support vector machine (SVM) models to classify six bacteria, which were cultured, centrifugated, washed and lyophilized. The identification rate of PCA-GA-ANN and PCA-GA-SVM reached 97.5% and 100%, respectively.[15] Rao *et al.* compared the spectra of graphite, slides and filter paper and found that the filter paper had the least interference on the LIBS spectrum. PCA was used to identify *Bacillus fusiformis*, *Pseudomonas koreensis*, *Bacillus subtilis*, *Bacillus thuringiensis* and *Escherichia coli*, which were obtained by centrifugal treatment after drying.[16] The above studies require complex sample preparation, such as thawing, rejuvenation, culture, centrifugation and lyophilization. It is more urgent to classify and identify bacteria directly, rapidly and effectively.

In this paper, we try to verify the identification rate of LIBS for bacteria in the case of simple sample pretreatment of bacteria through substrate optimization and an appropriate spectral analysis algorithm.

2 Experimental

2.1 Experimental setup

The experimental LIBS setup for bacterial identification is shown in Fig. 1. The Nd:YAG laser (Q-smart 450) produced 5 ns and 50 mJ pulses at 532 nm with a fixed repetition frequency of 1 Hz. The laser beam passed through a half-wave plate after being reflected by a mirror, and was then divided into two beams by using a polarizing beam splitting prism. The horizontally reflected laser entered a power meter, while the transmitted one was focused on the sample surface by using a convex lens ($f = 50$ mm) to generate plasmas. The plasma fluorescence

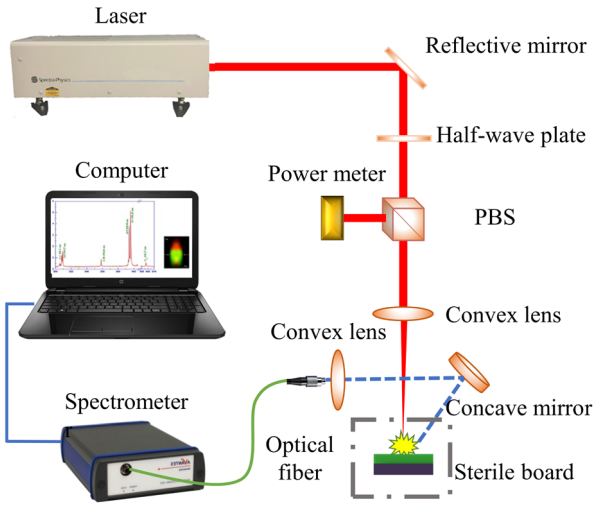

Fig. 1 Experimental LIBS setup for bacterial identification.

was converged into the optical fiber through a concave mirror and a plano-convex lens and transmitted to a four-channel spectrometer (AVASPEC-ULS4096CL-EVO) with a working wavelength of 192–1044 nm and resolution of 0.14–0.18 nm. All LIBS spectra were measured at 300 μs delay and 1 ms integration time. The samples were placed on an electronically motorized *X*–*Y* stage.

2.2 Bacteria samples

Six bacteria samples were used in the experiment, including *Escherichia coli* (ATCC25922, *E. coli*), *Enterococcus faecalis* (ATCC29212, *E. faecalis*), *Bacillus megaterium* (ATCC11107, *B. megaterium*), *Bacillus thuringiensis* (ATCC10792, *B. t*), *Pseudomonas aeruginosa* (ATCC9027, *P. aeruginosa*) and *Bacillus subtilis* (ATCC6633, *B. subtilis*). The sample pretreatment process was: after thawing for 30 minutes, a small amount of bacteria was diluted in 600 ml deionized water, and then placed on a clean workbench. After half an hour, 100 ml of the diluted strain was taken, smeared on a substrate as evenly as possible, and then dried naturally. In the experiment, five high-purity simple substances, graphite, silicon, aluminum, zinc and stannum, were used as substrates, and the best one was selected through spectral comparison for subsequent bacterial identification experiments.

2.3 Identification method

2.3.1 Spectral preprocessing. First, the effective spectra are selected according to the signal-to-noise (SNR) ratio of the spectral line. For example, if each spectrum contains 15 412 data, N groups of effective spectra of six samples will form a $N \times 15\,412$ matrix as the input matrix for training and testing of network. Then, the original matrix was normalized to the interval [0, 1] according to eqn (1), and PCA was used to reduce the dimension through linear projection.[17] In this way, fewer dimensions can retain most features of the original spectra without losing information. Assuming that the original feature

has only two dimensions, this method can centralize all the features and obtain a new set of feature values to replace the original. After obtaining the covariance matrix according to eqn (2), the eigenvalue λ of covariance matrix C and the corresponding eigenvector u can be obtained according to eqn (3):

$$x = (x - x_{\min})/(x - x_{\max}) \tag{1}$$

$$C = \begin{bmatrix} \mathrm{Cov}(x_1, x_1) & \mathrm{Cov}(x_1, x_2) \\ \mathrm{Cov}(x_2, x_1) & \mathrm{Cov}(x_2, x_2) \end{bmatrix} \tag{2}$$

$$Cu = \lambda u \tag{3}$$

At this time, each λ_i corresponds to a feature vector u_i. Sorting the feature values from large to small, selecting the largest first k eigenvalues and taking out the corresponding feature vectors, $\{(\lambda_1, u_1), (\lambda_2, u_2), \ldots, (\lambda_k, u_k)\}$ can be obtained. Here, the largest first k eigenvalues and corresponding eigenvectors are selected and projected as dimension reduction. For each sample X^i, the original eigenvalue is $({x_1}^i, {x_2}^i, \ldots, {x_k}^i)^T$, the new feature after projection is $({y_1}^i, {y_2}^i, \ldots {y_k}^i)^T$, and the calculation formula of the new feature is as follows:

$$\begin{bmatrix} {y_1}^i \\ {y_2}^i \\ \cdots \\ {y_k}^i \end{bmatrix} = \begin{bmatrix} {u_1}^T \cdot \left({x_1}^i, {x_2}^i, \ldots, {x_k}^i\right)^T \\ {u_2}^T \cdot \left({x_1}^i, {x_2}^i, \ldots, {x_k}^i\right)^T \\ \cdots \\ {u_k}^T \cdot \left({x_1}^i, {x_2}^i, \ldots, {x_k}^i\right)^T \end{bmatrix} \tag{4}$$

In this way, each sample X^i changes from the original $X^i = ({x_1}^i, {x_2}^i)^T$ to $X^i = {y_1}^i$, and the dimension reduction is completed.

2.3.2 Identification model. SVM is used to train and predict the data, because it can separate data samples by constructing hyperplanes, and thus effectively solve the linear classification and nonlinear classification problems.[18] The hyperplane constructed by SVM requires the distance between data points and the plane to be maximized as far as possible. By maximizing the classification interval, the fault tolerance rate can be increased, and the expected risk can be minimized, thus ensuring that the learning machine has better generalization ability. For the nonlinear inseparable problem in the input space, the vector points in the original data set can be transformed into a higher dimensional space through nonlinear mapping and an optimal separation hyperplane can be constructed to separate the nonlinear data on the plane which cannot be easily separated.

The original low-dimensional space samples are mapped to the high-dimensional feature space H, and there is a nonlinear mapping Φ: $R^d \rightarrow H$. SVM will use dot product $\langle \Phi(x_i) \cdot \Phi(x_j) \rangle$ to construct the classification plane in the high-dimensional space H, as shown in Fig. 2.

If there is a function K that makes $K(x_i, x_j) = \langle \Phi(x_i) \cdot \Phi(x_j) \rangle$, the specific form of Φ can be ignored and the dot product can be directly used in the high dimensional space H. Therefore, if the optimal classification plane can be constructed by the appropriate dot product function $K(x_i, x_j)$, linear classification in the high-dimensional feature space can be achieved through this nonlinear transformation, and the computational complexity is unchanged. The classification decision function can be expressed as:

$$f(x) = \mathrm{sign}\left(\sum_{i=1}^{N} a_i^* y_i K(x, x_i) + b^*\right) \tag{5}$$

where a_i is the Lagrange multiplier, if a^* is the optimal solution, the plane is the optimal classification plane, x_i is the standard support vector, b^* is the classification threshold, and K is the dot product kernel function, which usually includes the linear kernel function, polynomial kernel function and radial basis function. The corresponding expressions are listed in Table 1, where $\gamma = 1/2\sigma^2$, σ is the radius of the hypersphere, and d represents the kernel dimension. The linear kernel function can be selected when the data feature dimension is very high and the data are linearly separated with multiple samples. If the sample feature dimension is small and the sample number is normal, the Gaussian RBF kernel can be used. Compared with the Gaussian RBF kernel, the polynomial kernel function requires more parameters and has higher complexity. In addition, for polynomials with higher order, numerical calculation becomes difficult.

SVM can classify multi-class data by constructing multi-class classifiers, including all-together, one-against-one and one-against-all. The first one can modify the objective function directly, but it is complicated to consider all the categorical data when optimizing the formula. However, when the one-against-one is used for training, the total training and test time is relatively long in the case of many sample categories. Here, the one-against-all method is selected to classify the spectral data. In training, k kinds of samples are constructed into k training sets. The i-th classifier takes the i-th sample as the positive class ($y_i = +1$), and the rest as the negative class ($y_i = -1$). When making a decision, input x of a test sample and put it into k

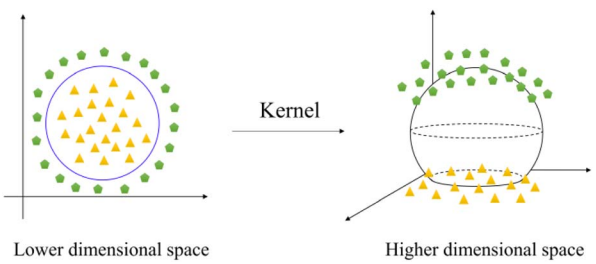

Fig. 2 Mapping from low dimensional space to high dimensional space.

Table 1 Common expression of kernel functions in SVM

Function	Expression
Linear kernel function	$K(x_i, x_j) = {x_i}^T x_j$
Polynomial kernel function	$K(x_i, x_j) = (\gamma {x_i}^T x_j + r)^d$, $\gamma > 0$
Gaussian radial basis function (RBF) kernel	$K(x_i, x_j) = \exp(-\gamma \lVert x_i - x_j \rVert^2)$, $\gamma > 0$

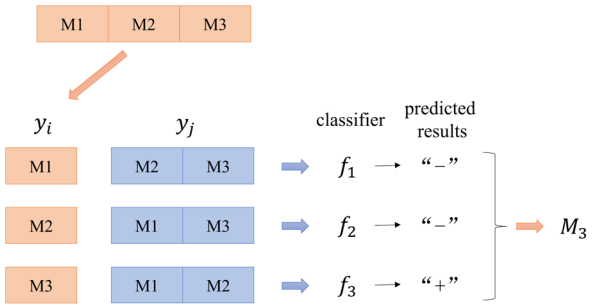

Fig. 3 One-against-all diagram of the three samples.

classifiers respectively. If only one classifier is predicted to be a positive class, the corresponding category is the final classification result. If multiple classifiers are predicted to be positive, the prediction confidence of the classifier is usually considered, and the category with the largest confidence is selected as the final classification result. The one-against-all diagram of the three samples is shown in Fig. 3.

2.3.3 Evaluation. Precision and recall are used to evaluate the prediction results of the model, where precision represents the proportion of the real positive samples among the positive samples predicted. There are two possibilities for positive prediction, one is to predict the positive class as the true positive (TP) class, and the other is to predict the negative class as the false positive (FP) class. Recall refers to the proportion of positive cases in the samples that are correctly predicted as positive cases. There are two possibilities, one is to predict the original positive class as positive (TP), and the other is to predict the original positive class as false negative (FN). The calculation formulae of precision and recall are:

$$\text{precision} = \frac{\text{TP}}{\text{TP} + \text{FP}} \tag{6}$$

$$\text{recall} = \frac{\text{TP}}{\text{TP} + \text{FN}} \tag{7}$$

The positive class predicted to be positive is defined as TP, the negative class predicted to be positive is defined as FP, the positive class predicted to be negative is defined as FN, and the negative class predicted to be negative is defined as TN.

3 Results and discussion

3.1 Substrate selection

In order to reduce the influence on the LIBS spectra of bacteria, a substrate with high purity, few spectral lines and low emission intensity should be selected. The LIBS spectra of high-purity graphite, silicon, aluminum, zinc and stannum are shown in Fig. 4. It can be seen that high-purity graphite best meets the

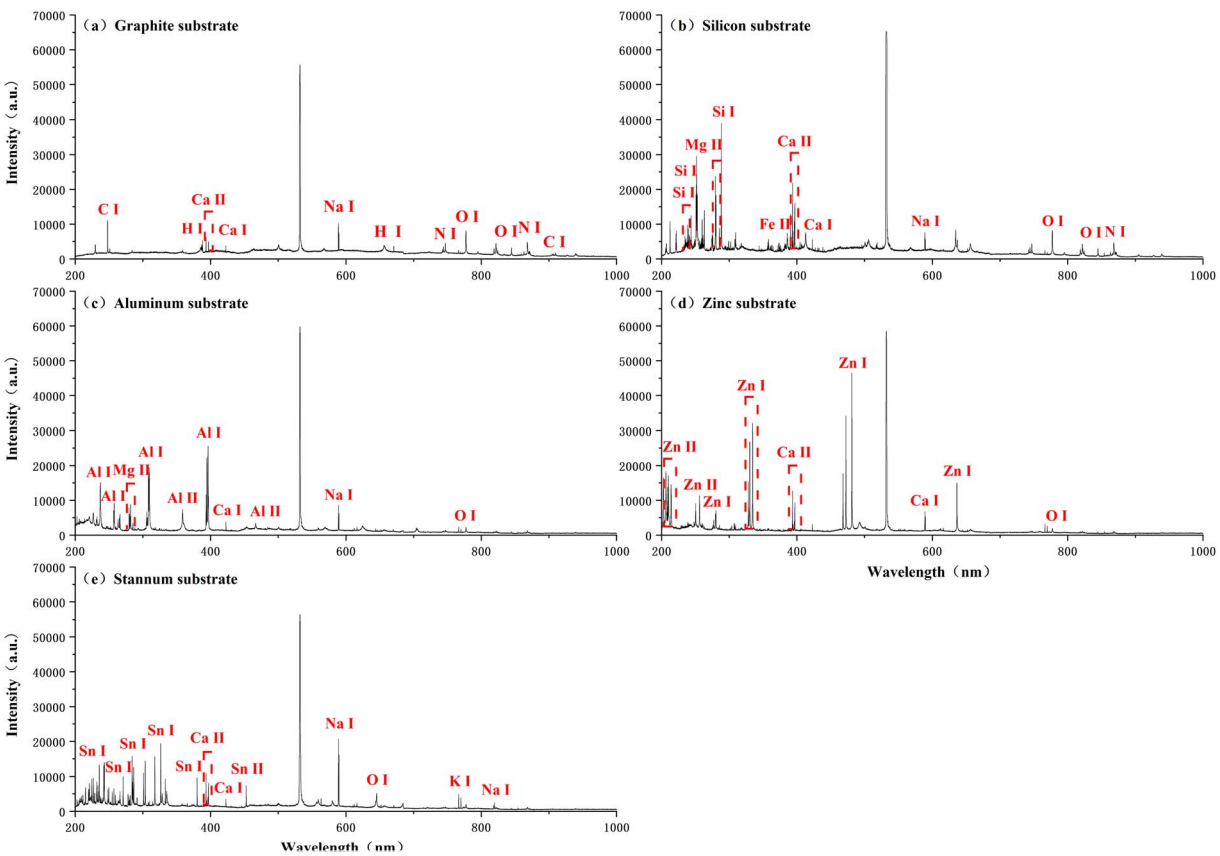

Fig. 4 LIBS spectra of five high-purity simple substances: (a) graphite, (b) silicon, (c) aluminum, (d) zinc and (e) stannum.

above requirements, so it was selected as the best substrate for subsequent measurements.[19,20]

3.2 Spectral preprocessing

In the experiment, 200 groups of LIBS spectra of each bacterium, including *E. coli*, *E. faecalis*, *B. megaterium*, *B. t*, *P. aeruginosa* and *B. subtilis*, were collected for investigation. In the bacterial spectra, the Na I 588.995 nm line has the most stable intensity and better SNR compared with other elemental spectral lines. Therefore, the SNR threshold of the Na I 588.995 nm line was set to 4.29 dB for screening, and 550 groups of effective spectra were obtained, as shown in Table 2. Here, 430 groups of these spectra were used as training sets, and the remaining 120 groups were used as prediction sets.

First, all the data were normalized, and then the dimensions of the training set data were reduced using PCA. For the training set, the first three principal components, PC1, PC2 and PC3, respectively, accounted for 70.98%, 13.13% and 2.22% of the total variance, with a cumulative variance of 86.33%. Fig. 5a shows the three-dimensional score plots of the first three PCs of all the bacteria. Fig. 5b shows the score of each PC, from which

Table 2 Number of training and prediction sets for the six bacteria

Bacteria	Original spectra	Effective spectra	Training sets	Prediction sets
E. coli	200	80	60	20
E. faecalis	200	73	60	13
B. megaterium	200	107	90	17
B. t	200	90	70	20
P. aeruginosa	200	92	70	22
B. subtilis	200	108	80	28
Total	1200	550	430	120

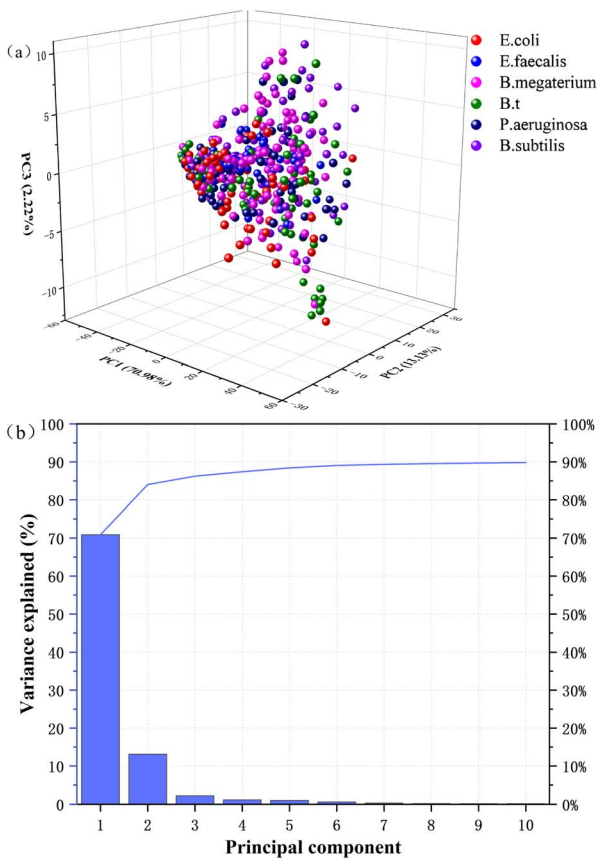

Fig. 5 Preprocessing of the six bacterial spectra with PCA: (a) three-dimensional scores of the first three PCs and (b) scores of each PC.

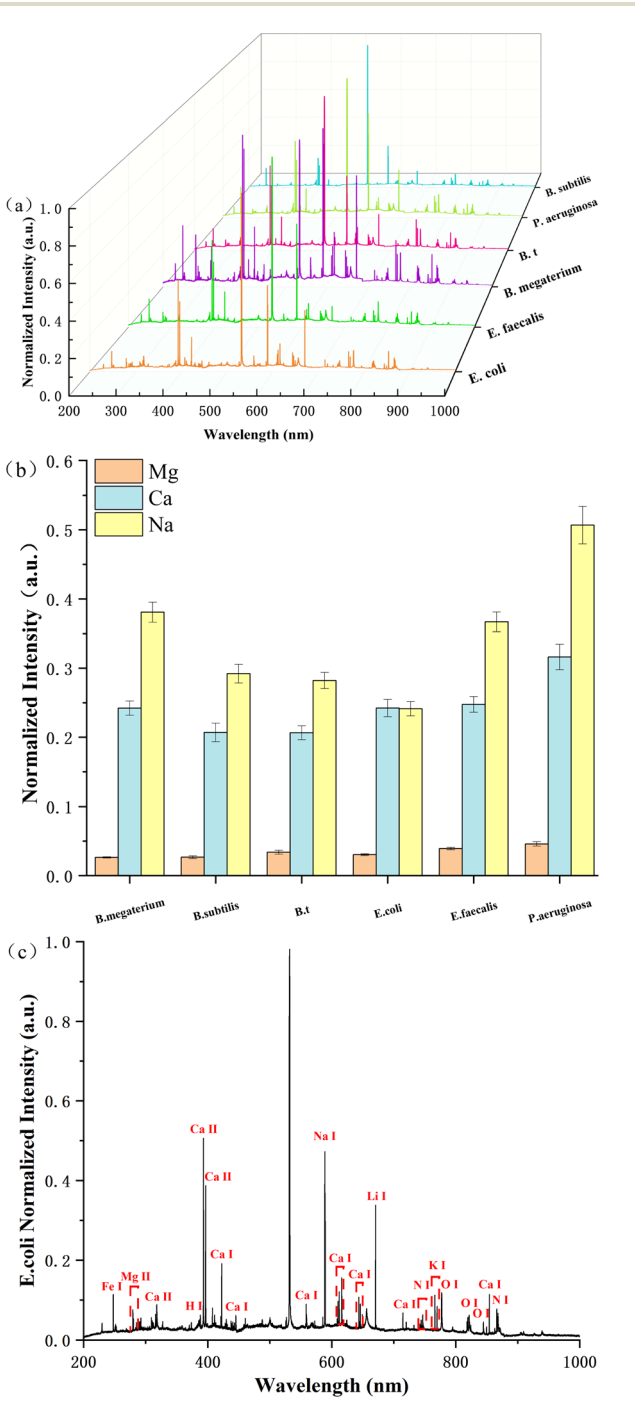

Fig. 6 LIBS spectra of the six bacteria, (b) normalized line intensities of Mg, Ca and Na, and (c) LIBS spectra of *E. coli*.

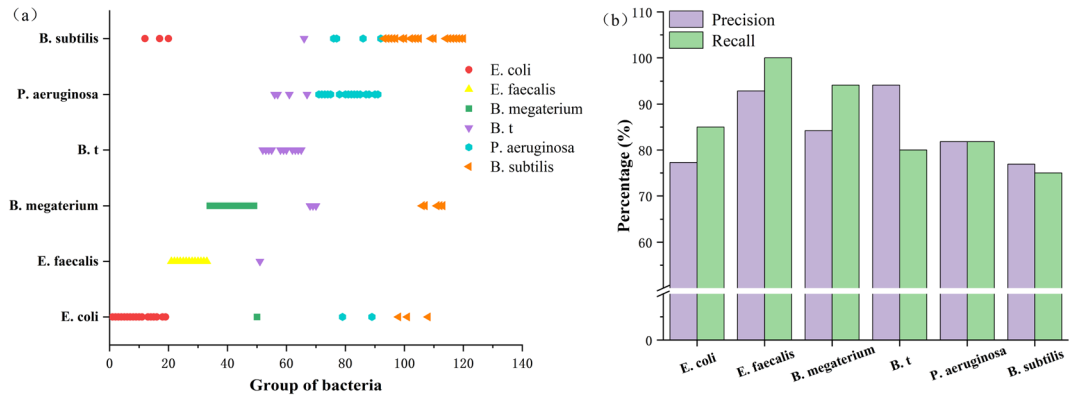

Fig. 7 (a) Identification results of the six bacteria and (b) the precision and recall.

it can be seen that the spectra of the six bacteria are clustered together. This is because the spectra of these bacteria are very similar, so they cannot be simply classified according to the first three PCs. After normalization and PCA preprocessing, the data dimension was reduced from 15 412 to 197, and the data were limited to the range of [0, 1], which greatly reduced the complexity of subsequent data processing.

Fig. 6 shows the LIBS spectra of the six bacteria and the normalized intensities of Mg, Ca and Na. It can be seen from Fig. 6a that the elemental emission lines in the LIBS spectra of the six bacteria are basically the same, with the main difference being the line intensity. Fig. 6b shows the normalized Mg II 279.5530 nm, Ca II 393.3661 nm and Na I 588.9950 nm lines in the spectra of the six bacteria, where the error bar represents the fluctuation of line intensity. For the six bacteria, the line intensity of Mg is roughly the same, while those of Ca and Na are slightly different. For example, in the spectrum of *E. coli* shown in Fig. 6c, in addition to the Mg II, Na I, Fe I, H I, O I and N I lines, the Ca I and Ca II lines are the most abundant. By comparing the bacterial spectrum with the substrate spectrum, it is worth mentioning that the spectral lines of H, O and N are mainly contributed by air, while those of Ca, Na, Mg, Fe, *etc.* mainly come from the cell wall of the bacteria. According to the Gram-staining method in microbiology and bacteriology, the bacterial species are classified into two groups, namely Gram-positive bacteria and Gram-negative bacteria. *E. coli* and *P. aeruginosa* belong to the latter, and the outer surface of the cell walls contains lipopolysaccharide (LPS). The core oligosaccharide structure in LPS is negatively charged as a whole, so it exists in the core oligosaccharide by combining with divalent ions such as calcium and magnesium. The cell wall of Gram-positive bacteria such as *B. subtilis*, *E. faecalis*, *B. t* and *B. megaterium* contains teichoic acid with a large number of negative charges on the molecule, which can concentrate magnesium around the cell to improve the activity of some synthetases on the cell membrane.[21] Compared with Fig. 4a, although there are Ca and Na lines in the spectrum of the graphite substrate, their intensity is much lower than that in the bacteria, so they can still be used as characteristic lines for bacterial identification. Unfortunately, due to the high similarity of these spectra, PCA, an unsupervised learning method, is still unable to completely identify these bacteria.

3.3 Bacterial identification

The process of using the SVM learning method to classify the six bacteria is as follows. First, the SVM classifier was built based on MATLAB, and the optimal kernel function and parameters were automatically found by the fitcecoc function in the libsvm toolbox, and the data were trained and predicted accordingly. Then, the prediction results of the model were evaluated by using the calculated precision and recall. In this work, the linear kernel function was selected, the box-constraint was 0.071, and the training method was one-against-all. Here 430 spectra were used for training, and the remaining 120 spectra were used for prediction. Fig. 7a shows the prediction results of the six bacteria, from which it can be seen intuitively that there are errors in the identification of some bacteria. The prediction precision and recall of each bacterium are shown in Fig. 7b, where the precision is 77.27%, 92.86%, 84.21%, 94.12%, 81.82% and 76.92%, and the recall is 85%, 100%, 94.12%, 80%, 81.82% and 75% respectively. The smaller the box-constraint, the higher the fault tolerance rate of data during training, the more the number of support vectors, and the stronger the generalization ability. The experimental results show that the correct number for classifying 120 groups of spectra of the six bacteria is 101, which corresponds to an identification rate of 84.17%.

4 Conclusions

In view of the time-consuming sample preparation required for traditional bacterial identification, such as thawing, rejuvenation, liquid culture, centrifugation and lyophilization, a new method for rapid bacterial identification using LIBS is proposed in this paper. By selecting high-purity graphite as a bacterial substrate, using spectral dimension reduction to preprocess and one-against-all linear kernel function SVM to model, the feasibility of rapid and direct identification of bacterial strains without sample preparation was verified. The experimental results show that the precision of *E. coli*, *E. faecalis*, *B. megaterium*, *B. t*, *P. aeruginosa* and *B. subtilis* is 77.27%, 92.86%, 84.21%, 94.12%, 81.82% and 76.92% respectively, their recall is 85%, 100%, 94.12%, 80%, 81.82% and 75% respectively, and the identification rate is 84.17%. It shows that this method can

preliminarily identify several low activity bacteria, but the identification rate is still limited due to the fluctuation of the LIBS spectra. The identification rate is still limited, which will be further improved by stabilizing the laser pulse energy and increasing the fluorescence collection efficiency.

Author contributions

Ziqi Mi is mainly responsible for the conceptualization, methodology, software and formal analysis of the experiment, and the writing of original draft. Yan Zhang and Lei Zhang are responsible for conceptualization and methodology, while Lei Zhang is also responsible for writing review and editing and project management. Jiahui Liang is responsible for investigation, software and formal analysis, and Fei Chen is responsible for validation, data curation and supervision. Shuqing Wang, Xiaofei Ma, Gang Wang, Wanfei Zhang, Zhenrong Liu, Xuebin Luo, Zefu Ye and Zhujun Zhu are responsible for providing the necessary resources for the experiment. Wangbao Yin and Suotang Jia are responsible for project management and funding acquisition, while Wangbao Yin is also responsible for writing review and editing.

Conflicts of interest

There are no conflicts to declare.

Acknowledgements

This work was supported by the National Key Research and Development Program of China (No. 2017YFA0304203); Changjiang Scholars and Innovative Research Team in University of Ministry of Education of China (No. IRT_17R70); National Natural Science Foundation of China (NSFC) (No. 61975103 and 61875108).

Notes and references

1 B.-D. Eitan, A. Brenner and A. Kushmaro, *Microb. Ecol.*, 2007, **54**, 439–451.
2 R. Knut, H. K. Gro, H. Ragnhild and T. R. Jan, *Food Microbiol.*, 2007, **24**, 474–481.
3 Y. Danting, Z. Haibo, H. Christoph, N. Reinhard and Y. Yibin, *Talanta*, 2016, **146**, 457–463.
4 S. Wei, L. Zhuo, Q. Baoling, G. Yue, W. Lili, W. Hai, H. Chengyan and Z. Bing, *Spectrosc. Spectral Anal.*, 2017, **37**(5), 1403–1407.
5 Y. Kalachyova, D. Mares, V. Jerabek, R. Elashnikov, V. Švorčík and O. Lyutakov, *Sens. Actuators, A*, 2019, **285**, 566–572.
6 Y. Wei, P. Kuankuan, C. Wei, M. Kexin, T. Chen, W. Xiangru and Y. Feng, *Chin. J. Anal. Chem.*, 2016, **44**(8), 1221–1226.
7 F. Ting, Z. Xin, L. Maogang, C. Tingting, J. Long, X. Yanyan, T. Hongsheng, Z. Tianlong and L. Hua, *Anal. Methods*, 2021, **13**, 3424–3432.
8 I. M. Qassem, S. Khadija, P. Sunil and J. R. Steven, *Appl. Opt.*, 2012, **51**, B99–B107.
9 L. G. Jennifer, C. L. Frank Jr, A. M. Chase and W. M. Andrzej, *Appl. Spectrosc.*, 2008, **62**, 353–363.
10 B. Matthieu, Y. Jin, B. Myriam, J. Julien, W. Jean-Pierre, A. Tanguy, F. Emeric and L. Patrick, *Appl. Phys. Lett.*, 2006, **89**, 163903.
11 B. Matthieu, G. Laurent, Y. Jin, W. Jean-Pierre, A. Tanguy, F. Emeric and L. Patrick, *J. Appl. Phys.*, 2006, **99**, 084701.
12 J. R. Steven, D. Jonathan and P. Sunil, *Spectrochim. Acta, Part B*, 2007, **62**, 1169–1176.
13 R. G. Gary, P. Bosoon, Y. Seung-Chul and C. L. Kurt, *Appl. Spectrosc.*, 2016, **70**, 494–504.
14 D. Marcos-Martinez, J. A. Ayala, R. C. Izquierdo-Hornillos, F. J. Manuel de Villena and J. O. Caceres, *Talanta*, 2011, **84.3**, 730–737.
15 Z. Yu, W. Qianqian, C. Xutai, T. Geer, W. Kai and L. Haida, *Appl. Opt.*, 2020, **59**, 1329–1337.
16 R. Gangfu, H. Lin, L. Muhua, C. Tianbing, C. Jinyin, L. Ziyi, X. Fanghao, Y. Hui, H. Xiuwen, Z. Huamao, L. Jinlong and Y. Mingyin, *Chin. J. Anal. Chem.*, 2018, **46**(7), 1122–1128.
17 A. M. Chase, C. L. Frank Jr, P. Thuvan, L. M. Kevin and W. M. Andrzej, *Spectrochim. Acta, Part B*, 2005, **60**, 1217–1224.
18 M. Arun Kumar and M. Gopal, *Expert Syst. Appl.*, 2011, **38**, 14238–14248.
19 W. A. Farooq, M. Atif, W. Tawfik, M. S. Alsalhi, Z. A. Alahmed, M. Sarfraz and J. P. Singh, *Plasma Sci. Technol.*, 2014, **16**, 1141–1146.
20 Y. Mingyin, L. JinLong, L. Muhua, L. Qiu, L. Zejian and H. Lin, Identification of *Escherichia coli* by laser induced breakdown spectroscopy, *2010 3rd International Conference on Biomedical Engineering and Informatics*, October, 2010.
21 J. R. Steven, J. Narmatha, D. Jonathan and P. Sunil, *J. Appl. Phys.*, 2009, **105**, 102034.